

# Reversal of the Hydrogen Bond to Zinc Ligand Histidine-119 Dramatically Diminishes Catalysis and Enhances Metal Equilibration Kinetics in Carbonic Anhydrase II<sup>†</sup>

Chih-chin Huang,<sup>‡</sup> Charles A. Lesburg,<sup>§</sup> Laura L. Kiefer,<sup>‡,||</sup> Carol A. Fierke,<sup>\*,‡</sup> and David W. Christianson<sup>\*,§</sup>

Department of Biochemistry, Duke University Medical Center, Box 3711, Durham, North Carolina 27710, and  
Department of Chemistry, University of Pennsylvania, Philadelphia, Pennsylvania 19104-6323

Received November 8, 1995; Revised Manuscript Received January 8, 1996<sup>®</sup>

**ABSTRACT:** Direct metal ligands to transition metals in metalloproteins exert a profound effect on protein–metal affinity and function. Indirect ligands, i.e., second-shell residues that hydrogen bond to direct metal ligands, typically exert more subtle effects on the chemical properties of the protein–metal complex. However, E117 of human carbonic anhydrase II (CAII), which is part of the E117–119–Zn<sup>2+</sup> triad, is a notable exception: E117-substituted CAIIs exhibit dramatically increased kinetics of zinc complexation, and the E117Q variant exhibits enormously diminished catalytic activity and sulfonamide affinity. The three-dimensional structures of zinc-bound and zinc-free E117Q CAII reveal no discrete structural changes in the active site that are responsible for enhanced zinc equilibration kinetics and decreased activity. Additionally, the structure of the acetazolamide complex is essentially identical to that of the wild-type enzyme despite the 10<sup>4</sup>-fold loss of enzyme–inhibitor affinity. We conclude, therefore, that the functional differences between E117Q and wild-type CAIIs arise from electrostatic and not structural differences in the active site. We propose that the E117Q substitution reverses the polarity of the residue 117–H119 hydrogen bond, thereby stabilizing H119 as a histidinate anion in the E117Q CAII holoenzyme. The additional negative charge in the first coordination sphere of the metal ion increases the pK<sub>a</sub> of the zinc–water ligand, destabilizes the transition state for CO<sub>2</sub> hydration, and facilitates the exchange of a zinc–histidine ligand with an additional water molecule by decreasing the stability of the tetrahedral zinc complex. These novel properties engineered into E117Q CAII facilitate the exploitation of CAII as a rapid and sensitive Zn<sup>2+</sup> biosensor.

As the prototypical zinc enzyme, human carbonic anhydrase II (CAII)<sup>1</sup> provides an extensively-studied and timely scaffolding for the dissection of structure–function relationships in a protein–zinc binding site. The structure of CAII from human blood has been determined by X-ray crystallographic methods (Liljas et al., 1972) and refined at 1.54 Å resolution (Håkansson et al., 1992). The active site of the enzyme is a cone-shaped cleft about 15 Å deep at the base of which resides a single zinc ion coordinated by the imidazole side chains of H94, H96, and H119, and hydroxide ion. Zinc-bound hydroxide is the catalytically-active nucleophile in the hydration of carbon dioxide to form

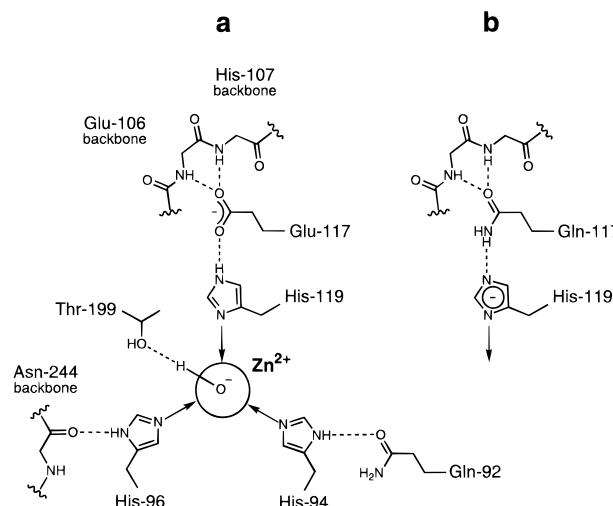


FIGURE 1: With respect to the E117–H119 hydrogen bond in the wild-type enzyme (a), the polarity of the Q117–H119 hydrogen bond in E117Q CAII (b) is proposed to be reversed.

<sup>†</sup> This work was supported by the Office of Naval Research and the National Institutes of Health (GM40602). C.A.L. is supported in part by NIH Cell and Molecular Biology Training Grant GM07229. Additionally, C.A.F. gratefully acknowledges the receipt of an American Heart Association Established Investigator Award and a David and Lucile Packard Foundation Fellowship in Science and Engineering.

\* Authors to whom correspondence should be addressed.

<sup>‡</sup> Duke University Medical Center.

<sup>§</sup> University of Pennsylvania.

<sup>||</sup> Present address: Glaxo Research Institute, V209, 5 Moore Dr., Research Triangle Park, NC 27709.

<sup>®</sup> Abstract published in *Advance ACS Abstracts*, March 1, 1996.

<sup>1</sup> Abbreviations: AZA, acetazolamide; CAI, human carbonic anhydrase I; CAII, human carbonic anhydrase II; CHES, 2-(N-cyclohexylamino)ethanesulfonic acid; E117Q, CAII variant with glutamine substituted for glutamate-117; EDTA, (ethylenedinitrilo)tetraacetic acid; MES, 2-(N-morpholino)ethanesulfonic acid; MOPS, 3-(N-morpholino)propanesulfonic acid; PAR, 4-(2-pyridylazo)resorcinol; PNPA, *p*-nitrophenyl acetate; TAPS, 3-[[tris(hydroxymethyl)methyl]amino]propanesulfonic acid; Tris, tris(hydroxymethyl)aminomethane.

bicarbonate ion and a proton (Coleman, 1967; Lindskog & Coleman, 1973; Silverman & Lindskog, 1988; Lindskog & Liljas, 1993). In the wild-type enzyme, the direct zinc ligands are fully saturated by hydrogen bond networks with second-shell residues (Figure 1a): H94 donates a hydrogen bond to the carboxamide side chain of Q92; H119 donates a hydrogen bond to the carboxylate side chain of E117; H96 donates a hydrogen bond to the backbone carbonyl oxygen

of N244; and zinc-bound hydroxide donates a hydrogen bond to the hydroxyl side chain of T199 (Håkansson et al., 1992). We refer to these second-shell residues as "indirect" zinc ligands, and such residues fine-tune protein–zinc affinity and function (Christianson & Alexander, 1989; Kiefer et al., 1995; Lesburg & Christianson, 1995). The His<sub>3</sub> site of CAII is exceptionally avid for zinc [ $K_d^{Zn} = 4$  pM; Lindskog & Nyman, 1964; Kiefer et al., 1993b].

Much research focuses on the zinc binding site of CAII, including the modification of the direct zinc ligands (Alexander et al., 1993; Kiefer et al., 1993a,b; Ippolito & Christianson, 1994; Kiefer & Fierke, 1994; Xue et al., 1994; Ippolito et al., 1995) and the indirect ligands (Kiefer et al., 1995; Lesburg & Christianson, 1995), as well as residues involved in the extensive hydrogen bond network involving zinc-bound solvent (Ippolito & Christianson, 1993; Krebs et al., 1993; Liang et al., 1993; Xue et al., 1993). With few exceptions (Ippolito et al., 1995), these studies result in variants with decreased catalytic activity and diminished protein–zinc affinity. Nevertheless, the properties of some of these variants allow for optimization of CAII-based metal ion biosensors (Thompson & Jones, 1993).

Here, we further investigate the role of indirect ligands in modulating the reactivity of bound zinc by characterizing the E117Q CAII variant using enzymological and X-ray crystallographic methods. This particular variant exhibits novel metal binding properties: the rate constant for zinc dissociation,  $k_{off}$ , is  $\geq 10^6$ -fold faster than that of the wild-type enzyme. However, the dissociation constant for zinc is increased only  $10^3$ -fold, suggesting that the association rate constant increases to the diffusion-controlled limit. Furthermore, this variant enzyme exhibits negligible catalytic activity, in surprising contrast with the behavior of other E117 variants previously studied (Kiefer et al., 1995; Lesburg & Christianson, 1995). These functional consequences of the E117Q substitution are all the more intriguing given that the substituted side chain is essentially isosteric with the wild-type side chain. Based on a combination of structural and biophysical studies of this variant, we conclude that Q117 stabilizes the negatively-charged histidinate form of H119 by reversing the hydrogen bond polarity between these two residues relative to that found between E117 and H119 in the wild-type enzyme (Figure 1b). Activity loss appears to arise exclusively from the electrostatic consequences of the E117Q substitution. Additionally, the enormous increase in zinc dissociation kinetics indicates an increase in the rate constant for zinc ligand exchange between histidine and bulk solvent due to destabilization of the histidine–zinc interaction by unfavorable ionization equilibria.

## MATERIALS AND METHODS

**Preparation of E117Q CAII.** The E117Q CAII variant was produced using oligonucleotide-directed mutagenesis of the cloned human CAII gene in pCAM (Krebs & Fierke, 1993), and the entire CAII gene was sequenced (Sanger et al., 1977). CAII was overexpressed in *Escherichia coli* BL21(DE3)pCAM by the addition of 0.25 mM isopropyl  $\beta$ -D-thiogalactopyranoside and then purified by sequential chromatography on DEAE-Sephacel and S-Sepharose media followed by a gel filtration column (PD-10, Pharmacia) (Alexander et al., 1993). The protein concentration was determined by absorbance using  $\epsilon_{280} = 54\,000\text{ M}^{-1}\text{ cm}^{-1}$  determined for wild-type CAII (Tu & Silverman, 1982).

**Catalytic Activity.** Initial rates of CO<sub>2</sub> hydration were measured by the changing pH-indicator method (Khalifah, 1971) in a KinTek stopped-flow apparatus at 24 mM CO<sub>2</sub>, 20  $\mu$ M E117Q CAII, 25  $\mu$ M *m*-cresol purple, 50 mM TAPS, pH 8.9 and 9.5, 25 °C, with ionic strength maintained at 0.1 M with Na<sub>2</sub>SO<sub>4</sub>. Background rates were subtracted from the observed rates. The initial rate of *p*-nitrophenyl acetate (PNPA) hydrolysis was monitored by absorbance,  $\epsilon_{348} = 5000\text{ M}^{-1}\text{ cm}^{-1}$  (Armstrong et al., 1966). The reaction was assayed under  $k_{cat}/K_M$  conditions at 50  $\mu$ M E117Q CAII, 0.5 mM PNPA in 40 mM buffer (CHES, pH 10.1, or TAPS, pH 9.0) with the ionic strength held constant at 0.08 M with Na<sub>2</sub>SO<sub>4</sub>. Background rates were measured in the presence of 2 mM acetazolamide.

**Zinc Affinity.** Free zinc was removed from CAII by chromatography on a Sephadex G-25M column (PD-10, Pharmacia). Then the enzyme (15–60  $\mu$ M) was dialyzed against a zinc/dipicolinate metal ion buffer (0–85  $\mu$ M total zinc/0.1–2 mM dipicolinate) in 10 mM Tris, pH 7.0. After incubating for 4 h at 30 °C, the enzyme concentration ( $[E]_{tot}$ ) was determined by the absorbance at 280 nm. The zinc concentration in the dialysate and enzyme sample was measured by the absorbance at 500 nm in the presence of 0.1 mM 4-(2-pyridylazo)resorcinol (PAR) and 4 M guanidine hydrochloride (Hunt et al., 1977; Kiefer & Fierke, 1994), and the enzyme-bound zinc ( $[E\cdot Zn]$ ) was quantified by the difference between the zinc concentration in the dialysate and in the enzyme sample. The concentration of free zinc was calculated from the dipicolinate–zinc stability constant (Sillén & Martell, 1964). The zinc dissociation constant ( $K_d^{Zn}$ ) was calculated using the Kaleidagraph (Synergy software) curve-fitting program with eq 1 where the end point,  $C$ , varied from 0.8 to 1.2.

$$[E\cdot Zn]/[E]_{tot} = C/(1 + K_d^{Zn}/[Zn]_{free}) \quad (1)$$

The zinc dissociation rate constant ( $k_{off}$ ) was estimated by diluting E117Q CAII into 10 mM Tris–sulfate, pH 7.0, 34 mM EDTA, immediately loading the sample onto a PD-10 column to remove unbound zinc and EDTA, and determining the concentration of bound zinc using the PAR assay (Kiefer & Fierke, 1994; Hunt et al., 1977). Additionally,  $k_{off}$  was measured by mixing E117Q CAII (3  $\mu$ M) in 10 mM Tris–sulfate, pH 7.0, with PAR (0.036–0.143 mM) in a KinTek stopped-flow spectrophotometer and observing the increase in absorbance at 490 nm reflecting the formation of a Zn(PAR)<sub>2</sub> complex (Hunt et al., 1985). The observed increase in absorbance is biphasic and is fit by eq 2 describing two independent exponential reactions.

$$\text{absorbance}_{490} = A_1 e^{-k_1 t} + A_2 e^{-k_2 t} + C \quad (2)$$

**Spectroscopy.** E117Q CAII apoenzyme was prepared by ultrafiltration against dipicolinate (Kiefer & Fierke, 1994), and then cobalt-substituted enzyme was prepared by the addition of a 4-fold molar excess of cobalt sulfate to apoenzyme. Optical absorption spectra were collected on 60  $\mu$ M Co<sup>2+</sup>-E117Q CAII in 10 mM buffer (Tris, pH 8.0, and CHES, pH 9.1 and 9.9) at 25 °C with the same concentration of Zn<sup>2+</sup>-enzyme in the reference cuvette. Under similar conditions, cobalt sulfate has an absorption maximum at 500 nm,  $\epsilon_{500} \approx 25\text{ M}^{-1}\text{ cm}^{-1}$ .

Table 1: Crystallographic Data Collection and Refinement Statistics for E117Q Carbonic Anhydrase II Structures

	holoenzyme	acetazolamide complex	apoenzyme
number of crystals	1	1	1
number of measured reflections	49 030	68 852	24 469
number of unique reflections	22 924	15 793	7 871
maximum resolution (Å)	1.8	2.0	2.5
minimum resolution (Å)	8.0	8.0	8.0
$R_{\text{sym}}^a$	0.069	0.033	0.078
Number of reflections used in refinement	18 728	15 323	7 328
Completeness of data (%)	92	93	90
$R_{\text{cryst}}^b$	0.177	0.164	0.166
number of water molecules in final cycle of refinement	139	151	41
rms deviation from ideal bond lengths (Å)	0.015	0.013	0.013
rms deviation from ideal bond angles (deg)	1.8	1.8	1.9
rms deviation from ideal dihedral angles (deg)	26.0	25.7	25.9
rms deviation from ideal improper angles (deg)	1.6	1.5	1.6

<sup>a</sup>  $R_{\text{sym}}$  for replicate reflections,  $R = \sum |I_h - \langle I_h \rangle| / \sum \langle I_h \rangle$ ;  $I_h$  = intensity measured for reflection  $h$ ;  $\langle I_h \rangle$  = average intensity for reflection  $h$  calculated from replicate data. <sup>b</sup> Crystallographic  $R$  factor,  $R = \sum ||F_o| - |F_c|| / \sum |F_o|$ ;  $|F_o|$  and  $|F_c|$  are the observed and calculated structure factors, respectively.

**Inhibitor Binding.** The acetazolamide (AZA) dissociation constant ( $K_d^{\text{AZA}}$ ) was determined by equilibrium dialysis; the enzyme (0–200  $\mu\text{M}$ ) in one compartment was equilibrated with tritium-labeled acetazolamide (1  $\mu\text{M}$ ) (Kandel et al., 1968) in a second compartment in 50 mM TAPS, pH 8.0, 0.2 mM zinc sulfate, 25 °C, with the ionic strength maintained at 0.1 M by  $\text{Na}_2\text{SO}_4$ . After reaching equilibrium (30 h incubation), the total acetazolamide concentration ( $[\text{AZA}]_{\text{tot}}$ ) was determined by the radioactivity, as quantified by scintillation counting, in the enzyme compartment. The enzyme-bound acetazolamide ( $[\text{E} \cdot \text{AZA}]$ ) was determined by the difference in radioactivity between the two compartments. The data were fit to a binding isotherm (see eq 1) using Kaleidagraph.

**Crystallography.** E117Q CAII was crystallized by the sitting-drop method: 5–10  $\mu\text{L}$  drops of precipitant buffer containing 50 mM Tris-HCl (pH 8.0 at 25 °C) and 50–75% saturated  $(\text{NH}_4)_2\text{SO}_4$  (1.75–2.5 M) were added to 5–10  $\mu\text{L}$  drops containing 0.3 mM protein and 50 mM Tris-HCl (pH 8.0 at 25 °C) in the crystallization well. The outer well contained 1 mL of precipitant buffer. Crystals grew as thin plates within 1 month at 4 °C; accordingly, 10 mM *n*-hexyl  $\beta$ -D-glucopyranoside was included in the crystallization wells to facilitate the formation of larger single crystals suitable for X-ray diffraction analysis (McPherson et al., 1986). Crystals were isomorphous with those of the native blood and recombinant wild-type enzymes and belonged to the monoclinic space group  $P2_1$  with unit-cell parameters  $a = 42.7$  Å,  $b = 41.7$  Å,  $c = 73$  Å, and  $\beta = 104.6^\circ$  (Liljas et al., 1972; Alexander et al., 1991).

In order to study the complex with the inhibitor acetazolamide, E117Q CAII crystals were soaked in a precipitant buffer solution containing 8 mM acetazolamide for 5 days prior to X-ray data collection.

Crystalline E117Q CAII apoenzyme was produced by transferring crystals to an artificial mother liquor containing 60% saturated  $(\text{NH}_4)_2\text{SO}_4$ , 50 mM Tris-HCl (pH 8.0 at 25 °C), and 10 mM dipicolinic acid. Crystals were allowed to equilibrate for 5 days at 25 °C, after which time the mother liquor was exchanged daily with a buffer solution of 60% saturated  $(\text{NH}_4)_2\text{SO}_4$ , 50 mM Tris-HCl (pH 8.0 at 25 °C), and 30 mM dipicolinic acid. Crystals were ready for data collection after a total of 3 weeks.

Crystals were mounted in 0.5 mm or 0.7 mm glass capillaries with a small portion of mother liquor and sealed

with wax. Intensity data were collected on an R-AXIS IIC image plate detector. Individual  $\phi$  oscillation images spanning either 2° or 3° were collected for 15 min each for a total sweep of 120°. A Rigaku RU-200HB rotating-anode X-ray generator provided Cu K $\alpha$  radiation at 124 kV/40 mA ( $\lambda = 1.5418$  Å). The crystal-to-detector distance was set to 9 cm, and the detector swing angle ( $2\theta$ ) was set to 0°. The crystal orientation matrix was initially obtained using REFIK (Kabsch, 1993), and reflections were subsequently integrated with MOSFLM (Nyborg & Wonacott, 1977). Data reduction was completed with CCP4 (French & Wilson, 1978; Collaborative Computing Project, 1994).

The starting coordinate set for the refinement of each E117Q CAII structure was that of wild-type CAII (Alexander et al., 1991) with the atoms of the Q117 side chain and all water molecules deleted from the model. In the refinement of the apoenzyme structure, the zinc ion was also removed from the initial coordinate set. Each structure was refined by simulated annealing with energy minimization as implemented in X-PLOR (Brünger et al., 1987). When the crystallographic  $R$ -factor dropped below 0.20 in each refinement, the variant side chain and water molecules (and inhibitor, in the acetazolamide complex) were modeled into electron density maps generated with Fourier coefficients  $2|F_o| - |F_c|$  and  $|F_o| - |F_c|$  and phases calculated from the in-progress atomic model. This work required the graphics software CHAIN (Sack, 1988), installed on a Silicon Graphics workstation.

During the refinement of each CAII variant, electron density maps were periodically calculated from the in-progress atomic model, and only minimal manual adjustments of atomic coordinates were found to be necessary. Refinement ultimately yielded structures with final crystallographic  $R$ -factors of 0.164–0.177 and excellent stereochemistry (Table 1).<sup>2</sup> The rms error in atomic positions for all CAII variants was estimated to be 0.15–0.20 Å by the method of Luzzati (1952). Electron density maps and coordinate superpositions shown in the figures were generated using MINIMAGE (Arnez, 1994) and/or MOLSCRIPT (Kraulis, 1991).

<sup>2</sup> Final coordinates have been submitted to the Brookhaven Protein Data Bank under Accession Codes 1ZSA, 1ZSB, and 1ZSC.

Table 2: Properties of E117Q CAII Compared to Wild-Type CAII

		wild-type	E117Q
PNPA hydrolysis	$k_{\text{cat}}/K_M$ ( $\text{M}^{-1} \text{s}^{-1}$ )	2500 <sup>a</sup>	3 <sup>b</sup>
CO <sub>2</sub> hydration <sup>c</sup>	$k_{\text{cat}}/K_M$ ( $\times 10^5 \text{M}^{-1} \text{s}^{-1}$ )	890 <sup>d</sup>	$0.02 \pm 0.02$
sulfonamide binding <sup>e</sup>	$K_d^{\text{AZA}}$ (mM)	0.008 <sup>d</sup>	$250 \pm 50$
zinc dissociation	$K_d^{\text{Zn}}$ (nM) <sup>f</sup>	0.004 <sup>g</sup>	$4.4 \pm 0.4$
	$k_{\text{off}}$ ( $\text{s}^{-1}$ ) <sup>h</sup>	$1.4 \times 10^{-6}$ <sup>i</sup>	$1.3 \pm 0.2$
$\text{p}K_a$ of zinc-bound water		6.9 <sup>g</sup>	$\geq 9.0$

<sup>a</sup> pH-independent  $k_{\text{cat}}/K_M$  taken from Krebs et al. (1991). <sup>b</sup> PNPA hydrolysis was increased  $\leq 10\%$  over the background rate at pH 10.1 by the addition of 50  $\mu\text{M}$  E117Q CAII. <sup>c</sup> Measured by the stopped-flow indicator method (Khalifah, 1971) in 50 mM TAPS, pH 8.9, ionic strength = 0.1 with  $\text{Na}_2\text{SO}_4$ , 25 °C. <sup>d</sup> Taken from Krebs et al. (1991). <sup>e</sup> Measured at pH 8.0, 25 °C. <sup>f</sup> Measured by equilibrium dialysis against zinc/dipicolinate buffers in 10 mM Tris-sulfate, pH 7.0, 30 °C. <sup>g</sup> Taken from Kiefer et al. (1993b). <sup>h</sup> Measured at pH 7.0, 25 °C. <sup>i</sup> Taken from Kiefer et al. (1995).

## RESULTS

**Catalysis and Sulfonamide Binding.** To delineate the effect of the E117Q substitution on the reactivity of zinc-bound hydroxide, we measured both the PNPA hydrolysis and CO<sub>2</sub> hydration activities (Table 2). At pH 10.1, the initial rate of PNPA hydrolysis is increased 10% over background by the addition of 50  $\mu\text{M}$  E117Q CAII, indicating that  $k_{\text{cat}}/K_M = 3 \text{M}^{-1} \text{s}^{-1}$ . No increase over background is observed at pH 9.0 ( $k_{\text{cat}}/K_M \leq 1 \text{M}^{-1} \text{s}^{-1}$ ). These data indicate that the esterase activity of E117Q CAII is decreased at least 800-fold compared to wild-type CAII (Table 2). Furthermore, since the pH dependence of the esterase activity directly reflects ionization of the zinc-bound water molecule in wild-type CAII (Coleman, 1967), the  $\text{p}K_a$  of the zinc-water ligand of E117Q is increased compared to wild-type CAII ( $\geq 9$  versus 6.9), suggesting that the E117Q substitution destabilizes the zinc-hydroxide species relative to zinc-water more than 100-fold. Additionally, the second-order rate constant for CO<sub>2</sub> hydration catalyzed by E117Q CAII at pH 8.9 is reduced by more than 5 orders of magnitude compared to wild-type CAII (Table 2). This decrease reflects both the increased  $\text{p}K_a$  of the zinc-bound water and the reduced stability of the transition state for CO<sub>2</sub> hydration in E117Q CAII.

Finally, to further probe the effects of the E117Q substitution on transition state structure, we measured a dissociation constant for acetazolamide, a putative transition state analog (Kumar et al., 1976), using equilibrium dialysis (Figure 2). These data clearly show that the E117Q substitution significantly decreases the affinity of CAII for [<sup>3</sup>H]acetazolamide; at 8.6  $\mu\text{M}$  enzyme, wild-type CAII binds  $\geq 96\%$  of the acetazolamide while E117Q CAII binds  $\leq 3\%$  of the acetazolamide. A fit of these data to a binding isotherm indicates that the affinity of E117Q CAII for acetazolamide is decreased more than  $10^4$ -fold compared to the wild-type enzyme (Table 2).

These properties of the E117Q CAII variant are not caused solely by disruption of the hydrogen bond with H119 since the catalytic activities of other indirect ligand variants at two positions (Q92  $\rightarrow$  A, N, E; and E117  $\rightarrow$  A, D) decrease only modestly (1.4–10-fold) and the  $\text{p}K_a$  values of zinc-bound water are within 1 unit of wild-type (Kiefer et al., 1995; Lesburg & Christianson, 1995). Furthermore, the dissociation constant for dansylamide, a fluorescent sulfonamide

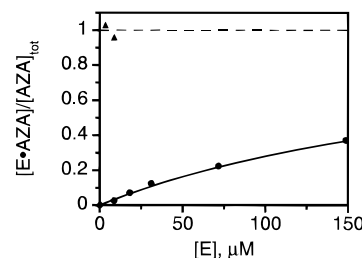


FIGURE 2: Measurement of an acetazolamide dissociation constant for E117Q CAII. 1 mL of CAII [0–200  $\mu\text{M}$ ; E117Q (●) or wild-type (▲)] was equilibrated with 1 mL of 1  $\mu\text{M}$  [<sup>3</sup>H]acetazolamide in an equilibrium dialysis chamber for 30 h in 50 mM TAPS, pH 8.0, 0.2 mM zinc sulfate at 25 °C with the ionic strength maintained at 0.1 M with sodium sulfate. The concentration of enzyme-bound acetazolamide ( $[\text{E} \cdot \text{AZA}]$ ) was calculated from the excess radioactivity in the enzyme compartment and the concentration of enzyme was calculated from the absorbance at 280 nm after equilibration. The data are fit to a binding isotherm assuming a stoichiometry of 1.

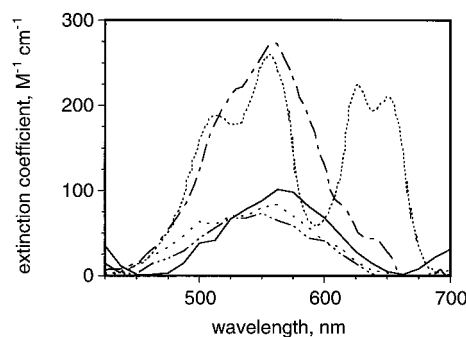


FIGURE 3: Optical absorption spectra of Co<sup>2+</sup>-substituted CAII. The spectra of Co<sup>2+</sup>-E117Q (60  $\mu\text{M}$  apoenzyme, 240  $\mu\text{M}$  cobalt sulfate) in 10 mM buffer [Tris, pH 8.0 (---); CHES, pH 9.1 (—); and CHES, pH 9.9 (···)] and Co<sup>2+</sup>-wild-type [MES, pH 5.5 (— — —), and CHES, pH 9.5 (— · —)]; taken from Kiefer et al., 1993a] were collected at 25 °C using identical concentrations of Zn<sup>2+</sup>-E117Q CAII in the reference cuvette. The molar absorptivities were calculated from the observed absorption and the concentration of CAII.

inhibitor (Chen & Kernohan, 1967), actually decreases 2–4-fold for the E117D and E117A CAII variants, respectively (K. A. McCall and C. A. Fierke, unpublished results). This suggests that substitution of a hydrogen bond acceptor (glutamate) with a hydrogen bond donor (glutamine) at position 117 causes a specific disturbance in the structure or electrostatic environment in the first coordination sphere of zinc that is not caused by substitution of the side chain with a water molecule. Intriguingly, the properties of E117Q CAII are reminiscent of CAII variants in which one histidine zinc ligand is replaced by a negatively-charged cysteine, aspartate, or glutamate (Kiefer & Fierke, 1994).

**Metal Binding.** Substitution of Co<sup>2+</sup> into the zinc binding site of CAII provides a useful spectroscopic probe of the composition and the geometric arrangement of the ligands about the metal ion (Bertini & Luchinat, 1983, 1984; Vallee & Galde, 1984). Figure 3 compares the optical absorption spectra of Co<sup>2+</sup>-substituted E117Q CAII at pH 8.0, 9.1, and 9.9 to the spectra of Co<sup>2+</sup>-wild-type CAII at low and high pH. The shape of the spectra of Co<sup>2+</sup>-E117Q CAII at all pH values resembles the spectra of the cobalt-water form of wild-type CAII in that there is one broad absorption peak centered at 560 nm ( $\epsilon \approx 100 \text{M}^{-1} \text{cm}^{-1}$ ). These spectra indicate that the cobalt-bound solvent molecule in Co<sup>2+</sup>-E117Q CAII does not ionize in this pH range, consistent

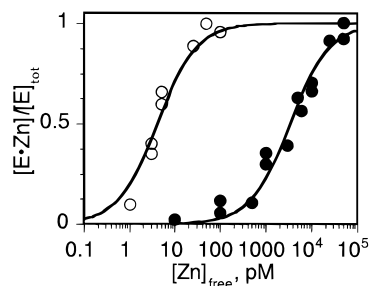


FIGURE 4: Measurement of a zinc dissociation constant for E117Q CAII. CAII apoenzyme (0.2 mL of 15–60  $\mu$ M) was dialyzed for 4 h at 30  $^{\circ}$ C against 0.5 L of a zinc sulfate (0–85  $\mu$ M)/dipicolinate (0.1–2 mM) metal ion buffer in 10 mM Tris, pH 7.0 [E117Q (●) and wild-type (○) (taken from Kiefer et al., 1993b)]. Enzyme-bound zinc was calculated as the excess zinc observed in the enzyme sample compared to the dialysate as quantified using a colorimetric assay (Hunt et al., 1977). The zinc dissociation constant was calculated from a fit of these data to eq 1 using the Kaleidagraph curve-fitting procedure.

with a significantly increased  $pK_a$  ( $\geq 9.9$ ). The decreased extinction coefficient of  $\text{Co}^{2+}$ -E117Q CAII may reflect a reduction in the concentration of a tetrahedral cobalt site due to either decreased affinity for cobalt, lessened stability of the protein, or an alternative geometry.

To assess the effect of the E117Q substitution on zinc affinity, we measured the zinc dissociation constant ( $K_d^{\text{Zn}}$ ) using equilibrium dialysis against a zinc/dipicolinate buffer (Figure 4; Kiefer & Fierke, 1994). The 1000-fold decrease in metal affinity of E117Q CAII compared to wild-type CAII at pH 7.0 (Table 2) is much larger than the 5–10-fold reductions observed for other variants with substituted indirect ligands (Kiefer et al., 1995).

Zinc equilibration kinetics for E117Q CAII similarly contrast with those measured for the wild-type enzyme, and as such, E117Q exhibits improved properties for real-time biosensor applications. We have previously demonstrated that the half-time for zinc dissociation from CAII ( $t_{1/2} = 5$  days; Kiefer & Fierke, 1994) is decreased up to 300-fold by the deletion of the hydrogen bond between E117 and H119 (Kiefer et al., 1995). To determine the half-time for zinc dissociation from E117Q CAII, we measured the zinc dissociation rate constant,  $k_{\text{off}}$ , by diluting E117Q CAII (50  $\mu$ M) into EDTA (34 mM in 10 mM Tris-sulfate, pH 7.0) to trap the dissociated zinc, by separating the CAII-bound zinc from free zinc using a gel filtration column (PD-10, Pharmacia), and by quantifying the bound zinc using a colorimetric assay (Kiefer & Fierke, 1994). After 4 min (the shortest possible time due to the transit time of the column), less than 4% of E117Q CAII contained a bound zinc, indicating that  $k_{\text{off}}$  is  $>0.01 \text{ s}^{-1}$  (an increase of more than  $10^4$ -fold compared to wild-type CAII). To more precisely measure  $k_{\text{off}}$ , we mixed E117Q CAII with the colorimetric zinc chelator, PAR, in a KinTek stopped-flow spectrophotometer and measured the increase in absorbance as a function of time (Figure 5). The observed kinetic transient is biphasic. The rate constant of the fast phase is dependent on the concentration of PAR [ $k_2 = (8 \pm 1) \times 10^4 \text{ M}^{-1} \text{ s}^{-1}$ ; data not shown], but slower than the rate constant for chelation of free zinc by PAR [ $(4.8 \pm 0.5) \times 10^5 \text{ M}^{-1} \text{ s}^{-1}$ ]. Furthermore, a transient with a rate constant equal to that of the fast phase is observed when wild-type CAII is mixed with PAR (Figure 5) under conditions where the active site zinc does not dissociate. Therefore, this fast phase likely

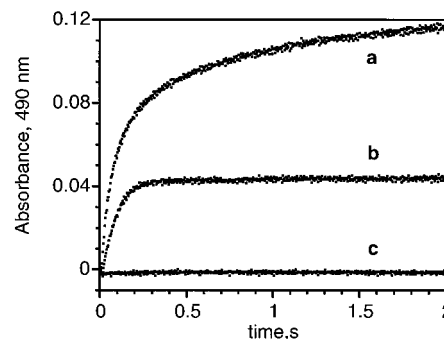


FIGURE 5: Measurement of the zinc dissociation rate constant from E117Q CAII. 10.5  $\mu$ M CAII (E117Q, line a; and wild-type, line b) in 10 mM Tris-sulfate, pH 7.0, was diluted 3.5-fold into 0.14 mM PAR in the same buffer. Line c shows the buffer alone diluted into PAR. The increase in absorbance as a function of time was collected, and the data were fit with an equation describing either a single exponential (line 2,  $k_1 = 12 \pm 1 \text{ s}^{-1}$ ) or two exponentials (eq 2) (line 3,  $k_1 = 14 \pm 1 \text{ s}^{-1}$ ;  $k_2 = 1.3 \pm 0.2 \text{ s}^{-1}$ ). The errors are derived from multiple measurements of these rate constants.

measures the rate constant for dissociation of zinc bound nonspecifically to CAII. Conversely, the observed rate constant of the slow phase ( $1.3 \pm 0.2 \text{ s}^{-1}$ ; Figure 5) is not dependent on the concentration of PAR or enzyme nor is a similar transient observed in the wild-type CAII or background controls, suggesting that this transient reflects the rate constant for dissociation of zinc from the active site of E117Q CAII. However, the amplitude of this phase,  $0.5 \pm 0.1$  mol of zinc/mol of enzyme, is less than expected, perhaps due to either complexation of zinc by other components of the reaction mixture or more rapid dissociation of a fraction of the active site zinc in E117Q CAII. Taken together, these data indicate that the rate constant for dissociation of zinc from E117Q CAII is increased more than  $8 \times 10^5$ -fold compared to wild-type CAII.

**Structure of the E117Q CAII Holoenzyme.** The neutral carboxamide side chain of the E117Q CAII variant is nearly isosteric with the negatively-charged carboxylate side chain of the wild-type enzyme; an electron density map is shown in Figure 6. The refined model superimposes almost perfectly upon the coordinates of the wild-type enzyme (Figure 7), and the rms deviation of  $C_{\alpha}$  coordinates is 0.24 Å. No significant structural differences are observed with the exception of occasional surface residues.

Since macromolecular X-ray crystallography cannot distinguish between oxygen and nitrogen atoms, the orientation of the Q117 carboxamide group must be inferred from the most reasonable constellation of possible hydrogen bonding interactions. Orienting the side chain such that the carboxamide oxygen accepts hydrogen bonds from the electro-positive backbone amide groups of E106 and H107 allows the side chain  $\text{NH}_2$  group to donate a hydrogen bond to the side chains of H107 (N–N separation = 2.8 Å) and H119 (N–N separation = 2.5 Å). Notably, this orientation of the Q117 side chain saturates all possible hydrogen bond interactions and reverses the polarity of the hydrogen bond with H119 relative to the wild-type enzyme. *Indeed, the side chain of H119 must be doubly deprotonated, i.e., as histidine anion, to accommodate the E117Q substitution (Figure 1b).*

The active site solvent structure in this variant is similar to that of the recombinant wild-type enzyme (Alexander et al., 1991). A spherical electron density peak centered 2.0

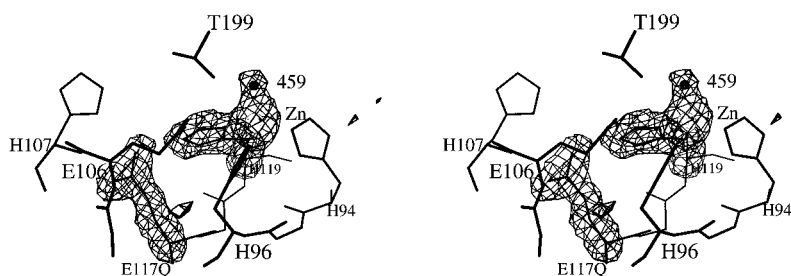


FIGURE 6: E117Q CAII holoenzyme. Difference Fourier ( $|F_o| - |F_c|$ ) electron density map contoured at  $3.5 \sigma$  in which the  $C_\alpha$  atoms and side chains of residues H119 and Q117,  $Zn^{2+}$ , and zinc-bound solvent (459) were omitted from the structure factor calculation.

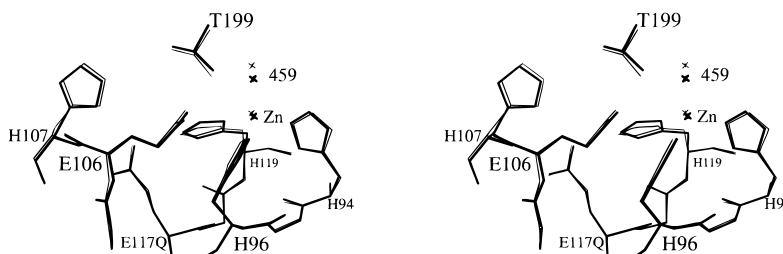


FIGURE 7: Least-squares superposition of E117Q CAII  $C_\alpha$  atoms (thick lines) with those of wild-type CAII (thin lines).

Å from zinc is interpreted as zinc-bound water (459), and this water molecule hydrogen bonds to the side chain of T199 ( $O^{459}-O_\gamma$  separation = 2.6 Å) as well as other solvent molecules (345 and 390) in the active site. Solvent 390 is the so-called “deep” water molecule located at the mouth of the substrate binding pocket (Lindskog, 1983) and must be displaced upon  $CO_2$  association. Importantly, no structural changes are observed in the substrate binding pocket.

Finally, in the E117Q CAII holoenzyme, H64 predominantly occupies the “out” conformation, with partial (30%) occupancy of the “in” position. In the native and wild-type enzymes, H64 predominantly occupies the “in” conformation above pH 6.5 (Alexander et al., 1991; Nair & Christianson, 1991; Håkansson et al., 1992). However, the “out” conformation does not compromise catalysis (Krebs et al., 1991).

**Structure of the E117Q CAII–Acetazolamide Complex.** The sulfonamide inhibitor acetazolamide is clearly visible in the electron density map (data not shown). Despite the  $10^4$ -fold diminished affinity of E117Q CAII toward acetazolamide, the inhibitor binds to this variant in a very similar binding mode to the complex with the wild-type enzyme (Vidgren et al., 1990). The side chain atoms of Q117 superimpose on the side chain atoms of the wild-type enzyme and on the E117Q holoenzyme. The side chain of H64 occupies the “out” position (Alexander et al., 1991; Nair & Christianson, 1991; Håkansson et al., 1992). The rms deviations of  $C_\alpha$  atomic positions between the E117Q/acetazolamide complex and other CAII structures range between 0.1 and 0.3 Å (data not shown). There are no significant structural differences from the wild-type structure in the vicinity of the binding pocket of acetazolamide; therefore, the  $10^4$ -fold loss of binding affinity must be due to electrostatic consequences of the E117Q substitution.

**Structure of the E117Q Apoenzyme.** Removal of zinc from E117Q CAII results in no significant structural changes relative to the holoenzyme (data not shown). Minor structural differences between the apoenzyme and holoenzyme are difficult to pinpoint due to the moderate resolution of this apoenzyme structure (2.5 Å). However, there are clear electron density peaks for active site solvent molecules and a notable lack of electron density due to a zinc ion. The

side chain atoms of Q117 are involved in identical hydrogen bond contacts as compared with the holoenzyme. In the active site, there is an 8 s peak within hydrogen bonding distance to  $N_\epsilon^{94}$ ,  $N_\epsilon^{96}$ ,  $N_\delta^{119}$ , and  $O_\delta^{199}$ . This electron density peak has been assigned to solvent molecule 327 and is located 1.3 Å from the position of the zinc ion in the wild-type enzyme (Alexander et al., 1991). This is consistent with the peak observed in the structure of the native apoenzyme (Håkansson et al., 1992). Although there is clear electron density for the side chain of H64 in the “out” position, there is significant density for some occupancy of the “in” conformation as well (Alexander et al., 1991; Nair & Christianson, 1991; Håkansson et al., 1992).

## DISCUSSION

There is precedent for histidinate–metal interactions in metalloenzymes; for instance, in copper,zinc-superoxide dismutase (Tainer et al., 1982), a negatively-charged histidinate side chain bridges the two active site metal ions. In addition, Smulevich and co-workers (1988a,b) detect equal populations of carboxylate–histidine–iron and carboxylic acid–histidine–iron triads in cytochrome *c* peroxidase using resonance Raman spectroscopy. Moreover, molecular orbital calculations on the D142–H69– $Zn^{2+}$  triad of carboxypeptidase A by Nakagawa and co-workers (1981) indicate a double potential energy minimum for the H69 proton, such that the D142-carboxylate–H69-histidine– $Zn^{2+}$  triad is in equilibrium with a D142-carboxylic acid–H69-histidine– $Zn^{2+}$  triad. Therefore, even in wild-type CAII, it is possible that the E117-carboxylate–H119-histidine– $Zn^{2+}$  triad is in equilibrium with the E117-carboxylic acid–H119-histidine– $Zn^{2+}$  triad. However, in the E117Q variant, it is clear that the Q117 amide side chain preferentially stabilizes the H119-histidinate– $Zn^{2+}$  interaction. This has profound effects on catalysis and protein–zinc equilibration kinetics, as discussed below. A similar polarity reversal has been proposed in the D102N variant of the serine protease trypsin where the activity is reduced 4 orders of magnitude (Craik et al., 1987; Sprang et al., 1987). These effects appear to arise more from the electrostatic, and not the structural, consequences of these substitutions.

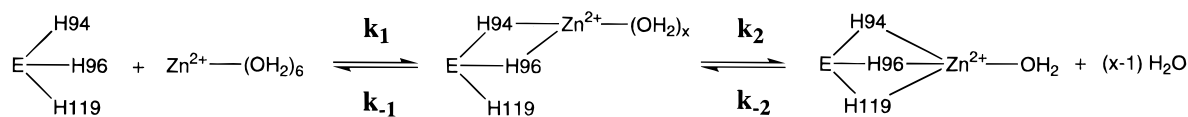


FIGURE 8: Schematic illustration of the wild-type CAII-Zn<sup>2+</sup> association pathway at neutral pH.

**Zinc-Bound Solvent and Catalysis.** The E117Q CAII holoenzyme and its acetazolamide complex reveal that neither transition-state binding nor proton transfer between zinc-bound solvent and H64 is structurally compromised by the essentially isosteric E117Q substitution. Furthermore, investigation of variants in which hydrogen bonds between protein side chains and histidine ligands are disrupted indicates that the catalytic efficiency and sulfonamide affinity of CAII are only modestly affected (Kiefer et al., 1995; Lesburg & Christianson, 1995; K. A. McCall and C. A. Fierke, unpublished results). Therefore, the surprising  $>10^3$ -fold loss of catalytic activity and the  $10^4$ -fold decrease in acetazolamide affinity must arise from the electrostatic consequences of the E117Q substitution. The most reasonable explanation of these data is that the E117Q substitution stabilizes the H119 zinc ligand as the negatively-charged histidinate anion in the holoenzyme. The stabilization of the histidinate anion [ $pK_a \approx 14$  in solution (Perrin, 1965) versus  $<8$  in the holoenzyme] is comparable to the stabilization of the zinc-bound hydroxide in wild-type CAII (Wooley, 1975). However, the formation of the negatively-charged histidinate ligand in the E117Q variant reduces the electrostatic stabilization of a second anion bound to zinc, thereby both elevating the  $pK_a$  of zinc-bound solvent and compromising its reactivity.

The substitution of negatively-charged ligands in the first coordination sphere of the metal typically elevates the zinc-water  $pK_a$  to greater than 8.6, an effect which is diagnostic of the magnitude of negative charge contributed by an engineered ligand, and decreases the pH-independent  $k_{cat}/K_M$  for CO<sub>2</sub> hydration  $10^2$ – $10^4$ -fold (Alexander et al., 1993; Kiefer et al., 1993a; Kiefer & Fierke, 1994). In E117Q CAII, the  $pK_a$  of zinc-bound water is greater than 9.0, which is consistent with the substitution of a negatively-charged direct metal ligand. Corresponding activity losses are greater than those observed in cysteine and aspartate variants of direct metal ligands H94 and H119 (Kiefer et al., 1995). These data indicate that a dominant factor in efficient catalysis of CO<sub>2</sub> hydration by CAII is electrostatic stabilization of the transition state by the positively-charged zinc ion; a diminution of the positive charge in the zinc binding site has dire consequences for catalytic efficiency. However, variants with a neutral ligand, such as glutamine, substituted for histidine retain reasonable catalytic activity (C.-C. Huang and C. A. Fierke, unpublished results).

**Zinc Binding.** The zinc-free and zinc-bound E117Q CAII structures reveal no significant differences, so no significant structural changes accompany zinc binding. Therefore, the  $10^3$ -fold decrease in zinc affinity likely reflects altered electrostatic interactions and the unfavorable ionization of the proposed histidinate in the E117Q holoenzyme.

In wild-type CAII, zinc not only binds tightly (4 pM) but the dissociation rate constant is also very slow ( $t_{1/2} = 5$  days; Kiefer & Fierke, 1994); amino acid substitutions at position 117 increase the zinc dissociation rate constant ( $k_{off}$ )  $10^2$ – $10^3$ -fold more than the dissociation constant ( $K_d^{Zn}$ ). Specifically, the observed rate constant for zinc association with

CAII ( $k_{on}$ ; estimated from the measured  $K_d^{Zn}$  and  $k_{off}$ ) is also increased from  $3.5 \times 10^5 \text{ M}^{-1} \text{ s}^{-1}$  (wild-type) to  $1 \times 10^7 \text{ M}^{-1} \text{ s}^{-1}$  (E117A),  $2.5 \times 10^7 \text{ M}^{-1} \text{ s}^{-1}$  (E117D), and  $3 \times 10^8 \text{ M}^{-1} \text{ s}^{-1}$  (E117Q) (Table 2; Kiefer et al., 1995). The slow zinc association rate for wild-type CAII suggests a two-step mechanism for the binding of zinc to wild-type CAII where the rate of formation of the metal complex is limited by an intramolecular step such as the dissociation of inner-sphere water molecules (Eigen & Hammes, 1963; Holyer et al., 1965, 1966). One possible mechanism for zinc association with wild-type consistent with the properties of first coordination sphere variants (Kiefer & Fierke, 1994) is the rapid formation of an initial complex in which zinc is coordinated to two protein ligands, e.g., H94 and H96, followed by the slow formation of the tetrahedral complex comprised of H94, H96, H119, and a solvent molecule ( $k_{on} = k_1 k_2 k_{-1}$ ; Figure 8). For E117 variants in general, the rate constants for ligand exchange increase significantly ( $k_2$ ,  $k_{-2}$ ). In the case of E117Q CAII, the diffusion-controlled formation of the intermediate complex becomes the rate-limiting step in zinc association ( $k_{on} = k_1$ ), and dissociation from this intermediate complex may also limit  $k_{off}$  ( $=k_{-1} k_{-2}/k_2$ ). The increased rate constant for zinc ligand exchange is not caused by structural differences between the E117Q and wild-type apoenzymes or holoenzymes; therefore, this increase reflects (1) the differing electrostatic environments in the zinc-bound complexes and (2) the decreased stability of the tetrahedral zinc complex resulting from the unfavorable protonation equilibria.

In closing, the lessons learned from this intriguing CAII variant have tremendous implications for the design of a zinc (or other metal) biosensor with extremely high affinity (i.e., sensitivity) and rapid equilibration kinetics. In particular, enhanced sensor-analyte association kinetics enable the development of a real-time CAII-based biosensor that can rapidly reequilibrate from one measurement to the next.

## ACKNOWLEDGMENT

We thank Eric Roush for the gift of [<sup>3</sup>H]acetazolamide and Keith McCall for stimulating discussions of this work.

## REFERENCES

- Alexander, R. S., Nair, S. K., & Christianson, D. W. (1991) *Biochemistry* 30, 11064–11072.
- Alexander, R. S., Kiefer, L. L., Fierke, C. A., & Christianson, D. W. (1993) *Biochemistry* 32, 1510–1518.
- Armstrong, J. M., Myers, D. V., Verpoorte, J. A., & Edsall, J. T. (1966) *J. Biol. Chem.* 241, 5137–5149.
- Arnez, J. G. (1994) *J. Appl. Crystallogr.* 27, 649–653.
- Bertini, I., & Luchinat, C. (1983) *Acc. Chem. Res.* 16, 272–279.
- Bertini, I., & Luchinat, C. (1984) *Adv. Inorg. Biochem.* 6, 71–111.
- Brünger, A. T., Kuriyan, J., & Karplus, M. (1987) *Science* 235, 458–460.
- Chen, R. F., & Kernohan, J. C. (1967) *J. Biol. Chem.* 242, 5813–5823.
- Christianson, D. W., & Alexander, R. S. (1989) *J. Am. Chem. Soc.* 111, 6412–6419.
- Coleman, J. E. (1967) *J. Biol. Chem.* 242, 5212–5219.

- Collaborative Computing Project, Number 4 (1994) *Acta Crystallogr. D50*, 760–763.
- Craik, C. S., Rocznik, S., Largman, C., & Rutter, W. J. (1987) *Science* 237, 909–913.
- Eigen, M., & Hammes, G. G. (1963) *Adv. Enzymol.* 25, 1–38.
- French, G. S., & Wilson, K. S. (1978) *Acta Crystallogr. A34*, 517–525.
- Håkansson, K., Carlsson, M., Svensson, L. A., & Liljas, A. (1992) *J. Mol. Biol.* 227, 1192–1204.
- Holyer, R. H., Hubbard, C. D., Kettle, S. F. A., & Wilkins, R. G. (1965) *J. Inorg. Chem.* 4, 929–935.
- Holyer, R. H., Hubbard, C. D., Kettle, S. F. A., & Wilkins, R. G. (1966) *J. Inorg. Chem.* 5, 622–625.
- Hunt, J. B., Rhee, M., & Storm, C. B. (1977) *Anal. Biochem.* 79, 614–617.
- Hunt, J. B., Neece, S. H., Schachman, H. K., & Ginsburg, A. (1985) *J. Biol. Chem.* 259, 14793–14803.
- Ippolito, J. A., & Christianson, D. W. (1993) *Biochemistry* 32, 9901–9905.
- Ippolito, J. A., & Christianson, D. W. (1994) *Biochemistry* 33, 15241–15249.
- Ippolito, J. A., Baird, T. T., McGee, S. A., Christianson, D. W., & Fierke, C. A. (1995) *Proc. Natl. Acad. Sci. U.S.A.* 92, 5017–5021.
- Kabsch, W. (1993) *J. Appl. Crystallogr.* 24, 795–800.
- Kandel, S. I., Wong, S.-C. C., Kandel, M., & Gornall, A. G. (1968) *J. Biol. Chem.* 243, 2437–2439.
- Khalifah, R. G. (1971) *J. Biol. Chem.* 246, 2561–2573.
- Kiefer, L. L., & Fierke, C. A. (1994) *Biochemistry* 33, 15233–15240.
- Kiefer, L. L., Ippolito, J. A., Fierke, C. A., & Christianson, D. W. (1993a) *J. Am. Chem. Soc.* 115, 12581–12582.
- Kiefer, L. L., Krebs, J. F., Paterno, S. A., & Fierke, C. A. (1993b) *Biochemistry* 32, 9896–9900.
- Kiefer, L. L., Paterno, S. A., & Fierke, C. A. (1995) *J. Am. Chem. Soc.* 117, 6831–6837.
- Kraulis, P. J. (1991) *J. Appl. Crystallogr.* 24, 946–950.
- Krebs, J. F., & Fierke, C. A. (1993) *J. Biol. Chem.* 268, 948–954.
- Krebs, J. F., Fierke, C. A., Alexander, R. S., & Christianson, D. W. (1991) *Biochemistry* 30, 9153–9160.
- Krebs, J. F., Ippolito, J. A., Christianson, D. W., & Fierke, C. A. (1993) *J. Biol. Chem.* 268, 27458–27466.
- Kumar, K., King, R. W., & Carey, P. R. (1976) *Biochemistry* 15, 2195–2202.
- Lesburg, C. A., & Christianson, D. W. (1995) *J. Am. Chem. Soc.* 117, 6838–6844.
- Liang, Z., Xue, Y., Behravan, G., Jonsson, B. H., & Lindskog, S. (1993) *Eur. J. Biochem.* 211, 821–827.
- Liljas, A., Kannan, K. K., Bergsten, P.-C., Waara, I., Fridborg, K., Strandberg, B., Carlbom, U., Jarup, L., Lovgren, S., & Petef, M. (1972) *Nature (London), New Biol.* 235, 131–137.
- Lindskog, S. (1983) in *Zinc Enzymes* (Spiro, T. G., Ed.) pp 78–121, John Wiley and Sons, New York.
- Lindskog, S., & Nyman, P. O. (1964) *Biochim. Biophys. Acta* 85, 462–474.
- Lindskog, S., & Coleman, J. E. (1973) *Proc. Natl. Acad. Sci. U.S.A.* 70, 2505–2508.
- Lindskog, S., & Liljas, A. (1993) *Curr. Opin. in Struct. Biol.* 3, 915–920.
- Luzzati, P. V. (1952) *Acta Crystallogr.* 5, 802–810.
- McPherson, A., Koszelak, S., Axelrod, H., Day, J., Williams, R., Robinson, L., McGrath, M., & Cascio, D. (1986) *J. Biol. Chem.* 1986, 1969–1975.
- Nair, S. K., & Christianson, D. W. (1991) *J. Am. Chem. Soc.* 113, 9455–9458.
- Nakagawa, S., Umeyama, H., Kitaura, K., & Morokuma, K. (1981) *Chem. Pharm. Bull.* 29, 1–6.
- Nyborg, J., & Wonacott, A. J. (1977) in *The Rotation Method in Crystallography* (Arndt, U. W., Wonacott, A. J., Eds.) pp 139–152, North-Holland, Amsterdam.
- Perrin, D. D. (1965) *Dissociation Constants of Organic Bases in Aqueous Solutions*, p 190, Butterworths, London.
- Sack, J. S. (1988) *J. Mol. Graphics* 6, 224–225.
- Sanger, F., Nicklen, S., & Coulson, A. R. (1977) *Proc. Natl. Acad. Sci. U.S.A.* 74, 5463–5467.
- Sillén, L. G., & Martell, A. E. (1964) *Stability constants of metal ion complexes, Special Publication No. 17*, p 546, The Chemical Society, London.
- Silverman, D. N., & Lindskog, S. (1988) *Acc. Chem. Res.* 21, 30–36.
- Smulevich, G., Mauro, J. M., Fishel, L. A., English, A. M., Kraut, J., & Spiro, T. G. (1988a) *Biochemistry* 27, 5486–5492.
- Smulevich, G., Mauro, J. M., Fishel, L. A., English, A. M., Kraut, J., & Spiro, T. G. (1988b) *Biochemistry* 27, 5477–5485.
- Sprang, S. T., Standing, T., Fletterick, R. J., Stroud, R. M., Finer-Moore, J., Xuong, N.-H., Hamlin, R., Rutter, W. J., & Craik, C. S. (1987) *Science* 237, 905–909.
- Tainer, J. A., Getzoff, E. D., Beem, K. M., Richardson, J. S., & Richardson, D. C. (1982) *J. Mol. Biol.* 160, 181–217.
- Thompson, R. B., & Jones, E. R. (1993) *Anal. Chem.* 65, 730–734.
- Tu, C. K., & Silverman, D. N. (1982) *Biochemistry* 21, 6353–6360.
- Vallee, B. L., & Galde, A. (1984) *Adv. Enzymol. Relat. Areas Mol. Biol.* 56, 283–430.
- Vidgren, J., Liljas, A., & Walker, N. P. (1990) *Int. J. Biol. Macromol.* 12, 342–344.
- Wooley, P. (1975) *Nature* 258, 677–682.
- Xue, Y., Liljas, A., Jonsson, B. H., & Lindskog, S. (1993) *Proteins: Struct., Funct., Genet.* 17, 93–106.
- Xue, Y., Jonsson, B. H., Liljas, A., & Lindskog, S. (1994) *FEBS Lett.* 352, 137–140.

BI9526692